Improving Periocular Recognition Accuracy: Opposite Side Learning Suppression and Vertical Image Inversion

Masakazu Fujio, Yosuke Kaga and Kenta Takahashi
Research and Development Group Hitachi Ltd., 292 Yoshida-cho, Totsuka-ku, Yokohama-shi, Japan
{*masakazu.fujio.kz, yosuke.kaga.dc, kenta.takahashi.bw*}*@hitachi.com*

Keywords: Periocular Recognition, CNN, Suppress Backpropagation.

Abstract: Periocular recognition has emerged as an effective biometric identification method in recent years, particularly when the face is partially occluded, or the iris image is unavailable. This paper proposes a deep learning-based periocular recognition method specifically designed to address the overlooked issue of simultaneously training left and right periocular images from the same person. Our proposed method enhances recognition accuracy by identifying the eye side, applying a vertical flip during training and inference, and stopping backpropagation for the opposite side of the current periocular. Experimental results on visible and NIR image datasets, using six different off-the-shelf deep CNN models, demonstrate an approximate 1∼2% improvement in recognition accuracies compared to conventional approaches that employ horizontal flip to align the appearance of the right and left eyes. The proposed approach's performance was compared with state-of-the-art methods in the literature on three unconstrained periocular datasets: CASIA-Iris-Distance, UBIPr. The experimental results indicated that our approach consistently outperformed the state-of-the-art methods on these datasets. From the perspective of implementation costs, the proposed method is applied during training and does not affect the computational complexity during inference. Moreover, during training, the method only sets the gradient values of the periocular image class of the opposite side to zero, thus having a minimal impact on the computational cost. It can be combined easily with other periocular authentication methods.

1 INTRODUCTION

In the era of rapidly evolving technology, biometric authentication has emerged as an essential security measure. Among various biometric modalities, facial recognition has been widely adopted due to its noninvasive nature and ease of implementation. However, the recent global pandemic has necessitated the use of facial masks, thereby obscuring significant parts of the face and hampering the effectiveness of facial recognition systems. This has prompted researchers to explore alternate biometric modalities that are resilient to such challenges. One such promising technique is periocular authentication. Such as periocular recognition focuses on the region around the eye, including the eyelashes, eyelids, and surrounding skin (Kumari and Seeja, 2022). Periocular recognition holds promise as it can be used even when the rest of the face is obscured, making it particularly relevant in the current context. Iris recognition is another method that has been considered, but it brings its own set of challenges. These include sensitivity to lighting conditions and the need for user cooperation in positioning the eye accurately for the scanner (Tan and Kumar, 2013).

Our study aims to explore and enhance the accuracy of periocular recognition as a viable alternative or complement to existing biometric techniques. We investigate a deep learning method in improving the accuracy of periocular recognition, particularly focusing on enhancing the discriminative capacity of resembling classes (the left and right periocular regions of the same individual). This, in turn, improves user authentication accuracy. Our approach involves applying a simple vertical image inversion and suppressing the learning of the opposite side periocular.

While it is also possible to train separate recognition models for the right eye and the left eye, the reduction in training samples could decrease the accuracy of identification.

The remainder of this paper is structured as follows: Section II contains a literature review, Section III presents the methodology and implementation method, Section IV presents the results, and finally, Section V provides the conclusion and future directions.

Fujio, M., Kaga, Y. and Takahashi, K.
Improving Periocular Recognition Accuracy: Opposite Side Learning Suppression and Vertical Image Inversion.
DOI: 10.5220/0013123400003912

In *Proceedings of the 20th International Joint Conference on Computer Vision, Imaging and Computer Graphics Theory and Applications (VISIGRAPP 2025) - Volume 2: VISAPP*, pages 298-305
ISBN: 978-989-758-728-3; ISSN: 2184-4321

2 RELATED WORK

Periocular recognition is a rapidly evolving field within biometrics, with numerous studies exploring different methodologies to improve recognition accuracy and robustness. In early works, researchers focused on hand-crafted descriptors such as Local Binary Patterns (LBP), Histogram of Oriented Gradients (HOG), and Scale-Invariant Feature Transform (SIFT) for feature extraction (Park et al., 2009) (Miller et al., 2010) (Adams et al., 2010) (Santos and Hoyle, 2012) (Ambika et al., 2017). These descriptors are designed to capture specific patterns within periocular images. For instance, Park et al. (Park et al., 2009) utilized these descriptors to prove the high discriminative nature of the periocular region under different conditions. Bharadwaj et al. (Bharadwaj et al., 2010) proposed a global description for periocular images using GIST and circular LBP operators, and Mahalingam and Ricanek (Mahalingam and Ricanek, 2013) implemented data alignment with the iris as the center for feature representation with multi-scale and patch-based LBP descriptors. These traditional methods, however, were found to be sensitive to various factors such as noise, rotation, and blur. To overcome these limitations, some researchers proposed the fusion of features from multiple descriptors or using novel descriptors that analyze images in a multi-resolution and multi-orientation manner (Cao and Schmid, 2016).

With the advent of deep learning, Convolutional Neural Networks (CNNs) have been increasingly employed for periocular recognition. CNNs have the advantage of automatically learning relevant features from data, leading to significant improvements in recognition accuracy. Researchers have explored various methods to improve the performance of CNNs in the field of periocular recognition. Zhao and Kumar (Zhao and Kumar, 2016) proposed a Semantics-Assisted CNN, which uses not only identity labels but also explicit semantic information such as gender and side information of the eyes for more comprehensive periocular feature extraction. Similarly, the ADPR model proposed by (Talreja et al., 2022) simultaneously jointly trains periocular recognition and soft biometrics prediction. In contrast with previous methods, their method fuses the predicted soft biometrics features with periocular features in the training step to improve the overall periocular recognition performance. Proença and Neves (Proenca and Neves, 2018) proposed Deep-PRWIS, a deep CNN model trained in such a way that the recognition is based exclusively on information surrounding the eye, with the iris and sclera regions features degraded during learning. Recent advancements have seen the fusion of hand-crafted and deep-learning methods to enhance periocular recognition performance. For instance, the Adaptive Spatial Transformation Networks proposed by (Borza et al., 2023) combines the advantages of both hand-crafted and deep learning features. The LDA-CNN model proposed by (Alahmadi et al., 2022) enhances periocular recognition by handling unconstrained variations such as illumination and pose. Their model incorporated an LDA layer after the last convolutional layer of the backbone model, then fine-tuned in an end-to-end manner. They evaluated the model using benchmark periocular datasets, indicating outperformed results than several state-of-the-art methods, even in difficult cross-conditions such as cross-eye and cross-pose.

Despite the considerable progress made by using deep learning methods, the literature overlooks the adverse effect of training left and right periocular images from the same person simultaneously. Our proposed method enhances recognition accuracy by identifying the eye side, applying a vertical flip during training and inference, and stopping backpropagation for the opposite side of the current periocular.

3 PROPOSED METHOD

A pivotal study examining the potential of employing the periocular region for human identification under various conditions is presented in (Park et al., 2009). Consistent with prior research (Park et al., 2009) (Kumari and Seeja, 2020) (Alahmadi et al., 2022), we consider each side of the periocular images as distinct identities. Subsequently, the user's identity is determined based on the authentication results or scores obtained from the left and right periocular images.

To amplify the number of training samples and enhance the precision of periocular authentication, we incorporate both left and right periocular features into a single Convolutional Neural Network (CNN) model. However, this approach raises several challenges concerning authentication accuracy. Specifically, it becomes more complex to differentiate the same individual's left and right periocular images compared to distinguishing another person's left or right periocular[1].

When training with the left periocular samples of

[1]The similarity scores of the left and right periocular images are lower than those of the right-to-right and left-to-left periocular images. However, they remain significantly higher than those of the periocular images of others, closely resembling identity pairs (Kumari and Seeja, 2020) (Alahmadi et al., 2022).

a given user (User1), treating the right-side periocular samples of the same user (User1) as general impostor samples (periocular images from other users) could potentially have adverse effects on the training of the right-side periocular classes for the same user. An alternative strategy could involve applying augmentation with a horizontal flip (Ahuja et al., 2016). Nonetheless, we propose that this approach may obscure the innate characteristics of the periocular region, blur the subtle differences between the right and left periocular images, and consequently reduce accuracy.

Prompted by these findings, we propose a novel CNN model training method designed to mitigate the adverse effects caused by training the other side of periocular classes. Our proposed method centers on two key approaches:

- Identify the left or right eye and apply a vertical flip during training and inferencing.
- Cease the backpropagation of the current periocular's opposite side.

By implementing these initial approaches, we expect that the model will easily distinguish periocular images of the same individual.

3.1 Overall Process of Periocular Recognition

Periocular authentication is a process that identifies individuals based on the distinctive features surrounding their eye region, including the eyelids, eyelashes, and eyebrows. The overall process of periocular CNN model training and inferencing, comprises the following steps:

[Training Phase]

Step 1: Region of Interest (ROI) Extraction. The Periocular images are extracted by using the OSS tools Media Pipe Facemesh[2].

Step 2: Image Preprocessing. If the input periocular image is from the left-side (or right-side), the image is flipped vertically.

Step 3: Data Augmentation. Data augmentation techniques (Chatfield et al., 2014) are employed to increase the number of training samples, excluding horizontal and vertical flips.

Step 4: Feature Extraction. Feature extraction is conducted using CNNs, such as Resnet18.

Step 5: Loss Calculation. The loss value is calculated using cross-entropy loss.

Step 6: Backpropagation. Perform backpropagation, excluding the opposite side of the current periocular (explained later).

[Inference Phase]

Step 1: ROI Extraction. Periocular images are extracted from facial images.

Step 2: Image Preprocessing. If the input periocular image is from the left-side (or right-side), the image is flipped vertically.

Step 3: Feature Extraction. Feature extraction is conducted using CNNs, such as Resnet18, without the final Fully Connected (FC) layer.

Step 4: Inferencing. The cosine similarity is calculated. Samples are accepted as genuine if the similarity is greater than or equal to a predefined threshold.

3.2 Image Preprocessing

As discussed in the previous subsection, our proposed method, in Step 2, flips the input images if they originate from a predefined side (either the left-side or the right-side). In our experiments, we compared the accuracies derived from three different scenarios: The first scenario does not involve any flips (Top); the second scenario involves a horizontal flip of the right periocular images (Middle); and the third scenario involves a vertical flip of the left periocular images (Bottom), as depicted in Fig.1.

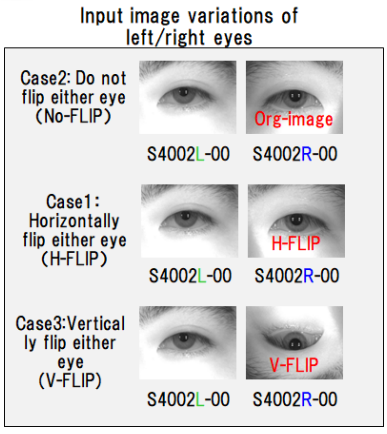

Figure 1: Variations of image flips. Top: w/o flips, Middle: horizontal flip of right perioculars, Bottom: vertical flip of left perioculars.

[2]https://nemutas.github.io/app-mediapipe-facemesh-demo/. We used following landmark IDs. Left: 244, 190, 56, 28, 27, 29, 30, 247, 226, 25, 110, 24, 23, 22, 232, 233, Right: 464, 414, 286, 258, 257, 259, 260, 467, 446, 255, 339, 254, 253, 252, 452, 453.

3.3 Training with Opposite Eye BackProp Suppression

As discussed in the previous subsection 3.1, our proposed method carries out backpropagation, except on the opposite side of the current periocular region (Step 6).

Fig. 2 depicts stopping the backpropagation for the opposite side of the current periocular region. The input image serves as an illustration of periocular images. The user ID ”002” corresponds to the user ID of the input image, while the side ID ”L” indicates whether the image originates from the right (”R”) or left (”L”) eye. The Convolutional Neural Network (CNN) model illustrates an inference model currently under training that accepts an image as input and yields features as output.

These features are utilized to estimate the user ID + side ID of the input image. The classifier can be composed of a fully connected layer, with the feature's dimensionality serving as the input dimension and the count of user ID + side ID types serving as the output dimension.

'Class logits' refers to the output vector produced by the classifier with dimensions corresponding to the user ID + side ID. The softmax function normalizes the class logits into probability values between 0 and 1. Class probability distribution signifies the distribution of vectors with a dimensionality equal to the number of user ID + side ID types.

The teacher probability distribution possesses a one-hot vector, where the correct data corresponding to user ID + side ID is marked as 1 and all other values are set to 0. Cross-entropy can be employed as a loss function to measure the discrepancy between the teacher and estimated class distribution.

The 'Target class' represents the input image's ID (user ID + side ID), while the 'Opposite side class' corresponds to the user ID + opposite side ID. The black dashed arrow illustrates the state of the backpropagation for the nodes corresponding to the user ID + side ID of the Target class. The gray dashed arrow depicts the state of the backpropagation for the nodes corresponding to the user ID + opposite side ID.

In Step 5, the discrepancy between the class and teacher probability distributions is computed. Subsequently, in Step 6, all gradients of the edges connected to the node of user ID + opposite side ID in the class logits are set to 0. Backpropagation for other nodes is then conducted as usual.

This methodology suppresses updates to parameters associated with user ID + side ID during the image learning phase for user ID + opposite side ID. Then, it enhances the estimation precision of the class ID for left and right periocular images in the post-training inference model.

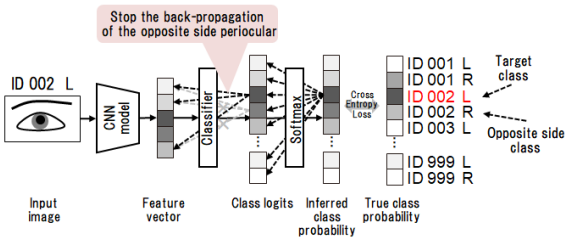

Figure 2: Outline of Training with Opposite Eye BackProp Suppression.

Algorithm 1 outlines the training process utilizing OEBS (Opposite Periocular BackProp Suppression). During each training iteration, a batch of samples X is initially passed through the CNN model to generate embeddings (F). These embeddings are then passed through the classifier to generate class logits (Y). Following this, the loss between the estimated class logit Y (class logits of the Y are normalized using a softmax operation in the *criterion* function) and the genuine one-hot labels y is calculated. Subsequently, the gradient of the edges connected to the node of user ID + opposite side ID within the class logits is set to '0.0', and backpropagation is performed as usual.

The proposed method is applied during training and does not affect the computational complexity during inference. Moreover, during training, the method only sets the gradient values of the periocular image class of the opposite side to zero, thus having a minimal impact on the computational cost.

4 EVALUATION

In this section, we assess the authentication accuracies of periocular recognition with and without our proposed method, which incorporates OEBS (Opposite Eye Backpropagation Suppression) and vertical image flips. To determine the efficacy of our method, we employ various state-of-the-art CNN models, including ResNet, SE-Resnet, and Mobilenet, among others, as described in the existing literature.

4.1 Database

We used four datasets to evaluate our method: one consists of IR face images (publicly available at CASIA-Iris-Distance, and the other comprises visible face images (purchased from the Datatang Face

Data: $X \in R^{T,B,C,W,H}$ images (T number of batches, B batch size, C channels, W width, H height), *model* CNN model, e epochs, y correct eye classes (one-hot encoding), y' opposite eye classes (one-hot encoding)
Result: trained CNN model
initialization;
for $i \leftarrow 0$ *to* e **do**
  for $j \leftarrow 0$ *to* T **do**
    $X \leftarrow D[j]$, $F \leftarrow$model(X),
     $Y \leftarrow$metric(F), $loss \leftarrow$criterion(Y, y)
    for $k \leftarrow 0$ *to* $len(y')$ **do**
      if $y'[k] = 1$ **then**
        model.fc.weight.grad[k] = 0
      end
    end
    ▷ Apply backprop.
  end
  if *No improvement in loss* **then**
    return *model*;
  else
    continue;
  end
end

Algorithm 1: Training with Opposite Eye Back- Prop Suppression.

Dataset[3]) and UBIPR (Proenca et al., 2010). These datasets span both visible and NIR spectrums. Further information about the databases used and the division of training and test sets is provided in Table 1.

Table 1: Summary of the employed databased for training and testing.

DB Name	CASIA-Iris -Distance	Datatang	UBIPr
# of subjects	142	4742	344
#. of classes	284	9484	688
#. of images	2,567	43,813	10,252
Resolution	2352 x1728	2976 x3968	500∼1000 x 400∼800
DB Type	Public	Paied	Public
Features	NIR	Visible	Visible
Train set	4,678	35,120	8,882
Test set	456	8,693	2,136

4.2 Recognition Accuracy: Periocular ID Evaluation

This section presents the tests' results to validate the proposed methods. Table 2∼4 provides a brief overview of the performance of various CNN models when evaluated on test data. For instance, the 'Model ' column denotes the name of the CNN models we used for the accuracy evaluation. We evaluated six different off-the-shelf DCNNs. The 'Method' column displays the method we introduced. 'Flip' refers to the types of image flips used, while the 'OEBS (Opposite Eye Backpropagation Suppression)' column indicates whether OEBS was utilized. 'H-flip,' 'NO-flip,' and 'V-flip' correspond to each image flip type as shown in Fig. 1. Then there are six (three × two) evaluation patterns in each CNN model. 'EER' stands for 'Equal Error Rate.' Each value in the Table represents the error rate (%) obtained under each setting. The underlined values signify the best result (minimum error) among each model's six evaluation patterns in each column (evaluation metrics). The boldface values indicate that the 'OEBS' method affected accuracy improvements.

Table 2: Comparison Results for the CASIA-IRIS-Distance. We employed EER (Equal Error Rate) (%) for the periocular ID.

Method		**Model Name**		
		resnet	**se-resnet**	**mobilenet**
Flip	OEBS	18	18	V2
V	w/o	3.06	3.57	2.61
	w/	**2.71**	**3.23**	3.36
H	w/o	12.89	3.37	3.09
	w/	**3.88**	4.55	3.86
NO	w/o	9.34	3.34	2.72
	w/	**2.77**	3.51	2.81

Table 3: Comparison Results for Datatang. We employed EER (Equal Error Rate) (%) for the periocular ID.

Method		**Model Name**		
		resnet	**se-resnet**	**mobilenet**
Flip	OEBS	18	18	V2
V	w/o	1.52	2.14	1.49
	w/	**1.50**	**1.54**	1.49
H	w/o	2.12	1.89	2.56
	w/	**1.90**	**1.62**	**2.38**
NO	w/o	2.11	1.49	1.64
	w/	**1.55**	**1.33**	**1.09**

When comparing the FLIP method, the H-flip approach consistently underperforms in each CNN model in each dataset as we expected. However, V-flip and NO-flip do not show clear superiority. In the UBIPR dataset, the NO-flip approach demonstrated better results than V-flip (2 out of 3 models in the UBIPR). There was a significant variation in the subject–camera poses (0-degree pose; 30-degree pose; -30-degree pose), so it may have been easier to distinguish between the left and right eye areas without flipping the image.

[3]https://datatang.co.jp/dataset/1402

Table 4: Comparison Results for UBIPR. We employed EER (Equal Error Rate) (%) for the periocular ID.

Method		Model Name		
		resnet	**se-resnet**	**mobilenet**
Flip	OEBS	18	18	V2
V	w/o	3.05	3.01	2.82
	w/	**2.65**	**2.83**	**2.45**
H	w/o	3.90	3.74	2.83
	w/	4.84	4.99	3.7
NO	w/o	2.51	2.28	2.26
	w/	**2.31**	2.85	**2.24**

Table 5: Comparison with separate network training. We employed EER (Equal Error Rate) (%) for the periocular ID. res:Resnet, seres:SeResnet, mn:Mobilenet.

Method		Model Name		
		res	**seres**	**mn**
DB	L/R	18	18	V2
CASIA-IRIS Distance	L	3.18	4.02	3.58
	R	4.42	3.82	5.18
Datatang	L	2.08	2.04	**2.21**
	R	1.89	1.94	**2.31**
UBIPR	L	4.16	4.63	3.58
	R	**3.38**	3.45	3.10

In the case of the OEBS method, for the CASIA-IRIS-Distance dataset, 4 out of 9 experimental settings (3 models $\times$ 3 flip types) exhibited positive effects (boldface characters); for the Datatang dataset, 8 out of 9 experimental settings exhibited positive effects, for the UBIPR dataset, 5 out of 9 experimental settings exhibited positive effects.

Figure 3, 4 and 5 shows the Roc curves for each database when using the SE-Resnet34 model. The x-axis stands for the FAR (False Acceptance Rate), and the y-axis stands for the TAR (True Acceptance Rate). The dashed gray line represents the EER (Equal Error Rate) points. From the Roc curves, we can also see that the NO-flip or the V-flip outperforms the H-flip. On the UBIPR dataset, the highest accuracy is achieved by V-flip/NO-flip with OEBS, followed by V-flip/NO-flip without OEBS. Next in accuracy are H-flip with OEBS, and lastly, H-flip without OEBS.

While it is also possible to train separate models for the right and the left periocular, the reduction in training samples could decrease the accuracy of identification. Table 5 shows the results with alternative strategies; separate network training. In some cases (with the MobilenetV2 (Datatang), with the Resnet (UBIPR)), separate network training approach outperforms the H-flip method. But for each database, the EER is worth than our methods (V-flip, NO-flip).

Using the samples from CASIA-IRIS-Distance, we will illustrate top-scoring imposter pair samples for each of the H-flip, NO-flip, and V-flip methods. Fig. 6 and Fig. 7 illustrate the examples of FA (False Acceptance) images. As expected, most high-scoring error instances in the H-flip method occur with pairs of left and right periocular images from the same user. On the other hand, in the case of the NO-flip and V-flip, most images are periocular images between different users.

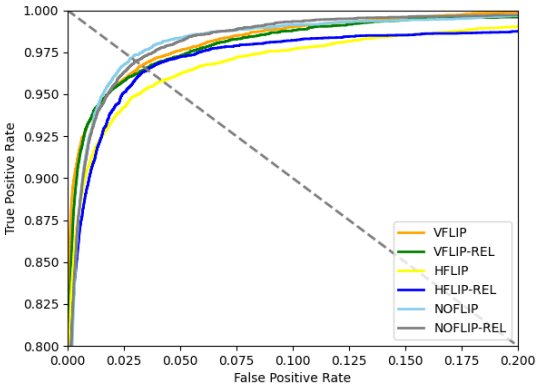

Figure 3: Roc curves of for CASIA-IRIS-Distance. Six experimental settings (3 fliptypes $\times$ 2 OEBS types) were trained with the SE-Resnet-34 model.

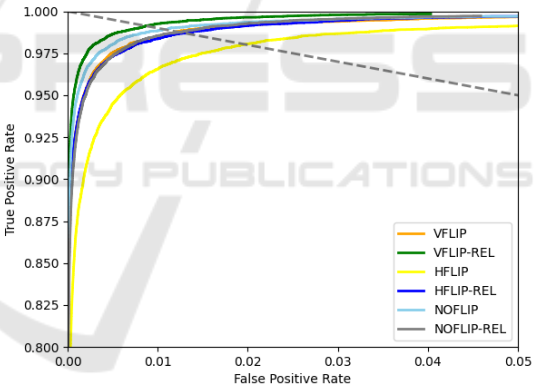

Figure 4: Roc curves of for Datatang.

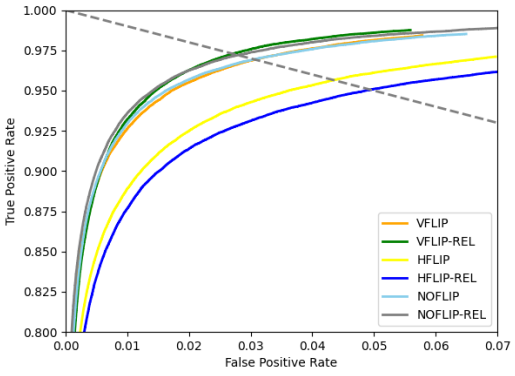

Figure 5: Roc curves of for UBIPR.

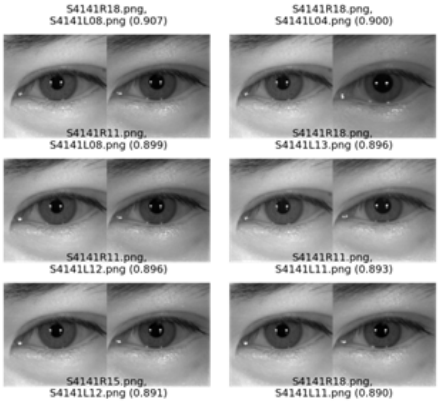

Figure 6: False Acceptance Examples with High Score: H-flip.

(a) NO-flip (b) V-flip

Figure 7: False Acceptance Examples with High Score.

4.3 Comparison with Other Existing Methods

The proposed approach's performance was compared with state-of-the-art methods in the literature on three unconstrained periocular datasets: CASIA Iris Distance, UBIPr, and UBIPR.v2. Following the same protocol (Kumari and Seeja, 2020) and (Zhou et al., 2024), 80% of the dataset was used for training, and the remaining 20% was used for testing all the datasets. Using SE-Resnet18 (with the NO-flip and the OEBS) as an example, we will demonstrate the performance of our proposed method.

Table 6 provides the identification result on CASIA Iris Distance (EER:0.65%) compared to (Zhao and Kumar, 2016), (Zou et al., 2022) and (Zhou et al., 2024). Table 7 compares the identification result of UBIPr (RANK1: 99.73%) to those of (Kumari and Seeja, 2020), and (Alahmadi et al., 2022).

From these results, it can be observed that our approach consistently outperformed the state-of-the-art methods on these datasets. Although there is some overlap in the confidence intervals in the Table 7, the superiority of the proposed method is generally recognized.

Table 6: Comparison with other existing methods: CASIA-Iris-Distance.

Method	EER(%)
(Zhao and Kumar, 2016)	6.61
(Zou et al., 2022)	7.74
(Zhou et al., 2024)	6.22
OURS	1.18

Table 7: Comparison with other existing methods: UBIPR.

Method	RANK1(%)
(Kumari and Seeja, 2020)	93.33 ± 1.06
(Alahmadi et al., 2022)	99.17 ± 0.39
OURS	99.73 ± 0.22

5 CONCLUSIONS

To improve the accuracy of the periocular authentication, we introduced two new methods that are designed to reflect the difference between the left and right periocular of the same person. Our proposed method employs two fundamental approaches to enhance periocular recognition. First, during training and inference, the system identifies whether an image is of the left or right eye and applies a vertical flip. Second, we stop backpropagation for the same individual's opposite side of the periocular region. In the experiments carried out on four datasets (visible and NIR images) with the six different off-the-shelf DCNNs, we achieved about $1 \sim 2\%$ improvements in the periocular recognition accuracies compared with the conventional horizontal flip approach. This was also true in the case of the user authentication evaluations (with score fusion of left and right periocular authentication scores). The proposed approach's performance was compared with state-of-the-art methods in the literature on three unconstrained periocular datasets: CASIA-Iris-Distance, UBIPr, and UBIPRv2. The experimental results indicated that our approach consistently outperformed the state-of-the-art methods on these datasets. From the perspective of implementation costs, the proposed method is applied during training and does not affect the computational complexity during inference. Moreover, during training, the method only sets the gradient values of the periocular image class of the opposite side of the same individual to zero, thus having a minimal impact on the computational cost. Furthermore, it can be combined easily with other periocular authentication methods. In future studies, we plan to extend this approach to other biometrics of left and right pairs or some dependent class pairs.

ACKNOWLEDGEMENTS

We want to acknowledge the support of the individuals at Hitachi-LG Data Storage and the Hitachi R&D members for sharing and providing us with the data for facial and periocular recognition experiments. Their contribution has been invaluable in advancing this research.

REFERENCES

Adams, J., Woodard, D. L., Dozier, G., Miller, P., Bryant, K., and Glenn, G. (2010). Genetic-based type ii feature extraction for periocular biometric recognition: Less is more. In *2010 20th International Conference on Pattern Recognition*, pages 205–208.

Ahuja, K., Islam, R., Barbhuiya, F. A., and Dey, K. (2016). A preliminary study of cnns for iris and periocular verification in the visible spectrum. In *2016 23rd International Conference on Pattern Recognition (ICPR)*, pages 181–186.

Alahmadi, A., Hussain, M., and Aboalsamh, H. (2022). Lda-cnn: Linear discriminant analysis convolution neural network for periocular recognition in the wild. *Mathematics*, 10(23).

Ambika, D., Radhika, K., and Seshachalam, D. (2017). Fusion of shape and texture for unconstrained periocular authentication. *International Journal of Computer and Information Engineering*, 11(7):831–837.

Bharadwaj, S., Bhatt, H. S., Vatsa, M., and Singh, R. (2010). Periocular biometrics: When iris recognition fails. In *2010 Fourth IEEE International Conference on Biometrics: Theory, Applications and Systems (BTAS)*, pages 1–6.

Borza, D. L., Yaghoubi, E., Frintrop, S., and Proenca, H. (2023). Adaptive spatial transformation networks for periocular recognition. *Sensors*, 23(5).

Cao, Z. and Schmid, N. A. (2016). Fusion of operators for heterogeneous periocular recognition at varying ranges. *Pattern Recognition Letters*, 82:170–180. An insight on eye biometrics.

Chatfield, K., Simonyan, K., Vedaldi, A., and Zisserman, A. (2014). Return of the devil in the details: Delving deep into convolutional nets.

Kumari, P. and Seeja, K. (2020). Periocular biometrics for non-ideal images: with off-the-shelf deep cnn and transfer learning approach. *Procedia Computer Science*, 167:344–352. International Conference on Computational Intelligence and Data Science.

Kumari, P. and Seeja, K. (2022). Periocular biometrics: A survey. *Journal of King Saud University - Computer and Information Sciences*, 34(4):1086–1097.

Mahalingam, G. and Ricanek, K. (2013). Lbp-based periocular recognition on challenging face datasets. *EURASIP Journal on Image and Video processing*, 2013:1–13.

Miller, P. E., Rawls, A. W., Pundlik, S. J., and Woodard, D. L. (2010). Personal identification using periocular skin texture. In *Proceedings of the 2010 ACM symposium on Applied Computing*, pages 1496–1500.

Park, U., Ross, A., and Jain, A. K. (2009). Periocular biometrics in the visible spectrum: A feasibility study. In *2009 IEEE 3rd International Conference on Biometrics: Theory, Applications, and Systems*, pages 1–6.

Proenca, H. and Neves, J. C. (2018). Deep-prwis: Periocular recognition without the iris and sclera using deep learning frameworks. *IEEE Transactions on Information Forensics and Security*, 13(4):888–896.

Proenca, H., Filipe, S., Santos, R., Oliveira, J., and Alexandre, L. (2010). The UBIRIS.v2: A database of visible wavelength images captured on-the-move and at-a-distance. *IEEE Trans. PAMI*, 32(8):1529–1535.

Santos, G. and Hoyle, E. (2012). A fusion approach to unconstrained iris recognition. *Pattern Recognition Letters*, 33(8):984–990.

Talreja, V., Nasrabadi, N. M., and Valenti, M. C. (2022). Attribute-based deep periocular recognition: Leveraging soft biometrics to improve periocular recognition. In *2022 IEEE/CVF Winter Conference on Applications of Computer Vision (WACV)*, pages 1141–1150.

Tan, C.-W. and Kumar, A. (2013). Towards online iris and periocular recognition under relaxed imaging constraints. *IEEE Transactions on Image Processing*, 22:3751–3765.

Zhao, Z. and Kumar, A. (2016). Accurate periocular recognition under less constrained environment using semantics-assisted convolutional neural network. *IEEE Transactions on Information Forensics and Security*, 12(5):1017–1030.

Zhou, Q., Zou, Q., Xuliang, G., Liu, C., Feng, C., and Chen, B. (2024). Low-resolution periocular images recognition using a novel cnn network. *Signal, Image and Video Processing*, 18:1–13.

Zou, Q., Wang, C., Yang, S., and Chen, B. (2022). A compact periocular recognition system based on deep learning framework attenmidnet with the attention mechanism. *Multimedia Tools Appl.*, 82(10):15837?15857.